Science of the Total Environment 945 (2024) 174130

Contents lists available at ScienceDirect

Science of the Total Environment

journal homepage: www.elsevier.com/locate/scitotenv

Greening of Svalbard

Stein Rune Karlsen [a,*], Arve Elvebakk [b], Laura Stendardi [c], Kjell Arild Høgda [a], Marc Macias-Fauria [d]

[a] NORCE Norwegian Research Centre AS, P.O. Box 6434, N-9294 Tromsø, Norway
[b] The Arctic University Museum of Norway, UiT – The Arctic University of Norway, N-9037 Tromsø, Norway
[c] Institute for Earth Observation, Eurac Research, Viale Druso 1, 39100 Bolzano, Italy
[d] Scott Polar Research Institute, University of Cambridge, Cambridge CB2 1ER, United Kingdom

HIGHLIGHTS

- A rapid recent greening of Svalbard closely linked to temperature increase.
- Record-high tundra productivity in Svalbard in 2022
- A new method that shows high temperature – vegetation productivity correlations
- Decline in sea-ice extent increases tundra productivity.

GRAPHICAL ABSTRACT

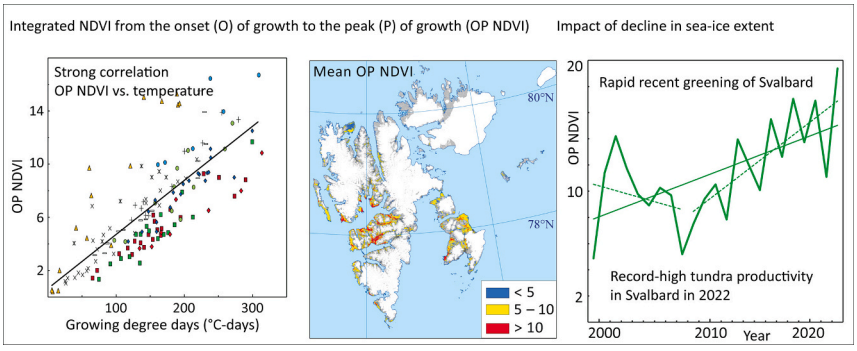

ARTICLE INFO

Editor: Frederic Coulon

Keywords:
Greening of the tundra
Growing degree days
Onset of growth
Vegetation productivity
MODIS
NDVI
Svalbard

ABSTRACT

Svalbard, located between 76°30′N and 80°50′N, is among the regions in the world with the most rapid temperature increase. We processed a cloud-free time-series of MODIS-NDVI for Svalbard. The dataset is interpolated to daily data during the 2000–2022 period with 232 m pixel resolution. The onset of growth, with a clear phenological definition, has been mapped each year. Then the integrated NDVI from the onset (O) of growth each year to the time of average (2000–2022) peak (P) of growth (OP NDVI) have been calculated. OP NDVI has previously shown high correlation with field-based tundra productivity. Daily mean temperature data from 11 meteorological stations are compared with the NDVI data. The OP NDVI values show very high and significant correlation with growing degree days computed from onset to time of peak of growth for all the meteorological stations used. On average for the entire Svalbard, the year 2016 first had the highest greening (OP NDVI values) recorded since the year 2000, then the greening in 2018 surpassed 2016, then 2020 surpassed 2018, and finally 2022 was the year with the overall highest greening by far for the whole 2000–2022 period. This shows a rapid recent greening of Svalbard very strongly linked to temperature increase, although there are regional differences: the eastern parts of Svalbard show the largest variability between years, most likely due to variability in the timing of sea-ice break-up in adjacent areas. Finally, we find that areas dominated by manured moss-tundra in

* Corresponding author.
E-mail addresses: skar@norceresearch.no (S.R. Karlsen), arve.elvebakk@uit.no (A. Elvebakk), Laura.Stendardi@eurac.edu (L. Stendardi), kjho@norceresearch.no (K.A. Høgda), mm2809@cam.ac.uk (M. Macias-Fauria).

https://doi.org/10.1016/j.scitotenv.2024.174130
Received 27 February 2024; Received in revised form 16 June 2024; Accepted 17 June 2024
Available online 21 June 2024

the polar desert zone require new methodologies, as moss does not share the seasonal NDVI dynamics of tundra communities.

1. Introduction

The Arctic has warmed nearly four times faster than the rest of the world over the past 4 decades (Rantanen et al., 2022). This means that the region is on average ~3 °C warmer than it was in 1980. Exceptional warming has occurred over the northern Barents Sea area, where the High Arctic Svalbard Archipelago is located, due to the strong decline in sea ice cover. Isaksen et al. (2022) reported temperature increases of up to 2.7 °C per decade at the isolated island Karl XII-øya, located at 80°39′N, north of the major islands of the north-eastern part of the archipelago. This warming is unprecedented in this region and exceptional in the Arctic and even on a global scale.

The importance of summer temperatures for Arctic (and especially High Arctic) plant growth and distribution is well known (e.g., Elmendorf et al., 2012; Walker et al., 2005). In Svalbard, a high correlation between measurements of vegetation growth and June–July temperatures is found (van der Wal and Stien, 2014). From a broad-scale bioclimatic zonation study in arctic Canada, Edlund and Alt (1989) concluded that environmental factors other than summer temperatures were almost insignificant by comparison. Further illustrating the strong relationship between vegetation and temperature in the Arctic, Karlsen and Elvebakk (2003) showed that the distribution of vascular plants in a topographically diverse study area in Greenland could be used to map in detail the local climatic mosaic in terms of growing season temperatures. However, the response of vegetation to higher temperatures has been shown to be mediated by other factors as well, most notably the hydrological conditions (Campbell et al., 2021; Myers-Smith et al., 2015).

Most studies based on time-series of satellite-derived vegetation indices (such as the Normalised Difference Vegetation Index, NDVI (Tucker, 1979) show that the Arctic and adjacent boreal areas have experienced increased vegetation growth and become “greener”, a phenomenon linked to increased tundra plant productivity (e.g., Raynolds et al., 2012; Walker et al., 2011) and shown to have been primarily driven by rising temperatures due to climate change (Beck and Goetz, 2011; Berner et al., 2020; Epstein et al., 2012; Jeganathan et al., 2014; Myneni et al., 1997; Park et al., 2016; Vickers et al., 2016; Wang and Friedl, 2019; Xu et al., 2013).

However, this trend is not uniform. Spatial heterogeneity in the greening signal is largest in the High Arctic, which is attributed to lower plant cover and diversity restricting in part the biological response to warming (Berner et al., 2020) or to local-to-regional controls on temperature by sea ice dynamics (Macias-Fauria et al., 2017), and some areas experience a ‘browning trend’ (e.g., Phoenix and Bjerke, 2016), also more frequent in the High Arctic (Berner et al., 2020). Temporal heterogeneity has also been reported, with declines in the correlation between timeseries of growing season air temperatures and NDVI across the pan-Arctic (Piao et al., 2014) and in Svalbard in particular (Vickers et al., 2016). Moreover, when interpreting spectral greening signals, it can be challenging to distinguish ecological changes from differences due to methods and sensor/platform-related issues (Myers-Smith et al., 2020). Trends in NDVI data produced from different satellite datasets or by use of different methods do not always correspond at a given location (Guay et al., 2014). This is particularly challenging in the High Arctic. At such high latitudes (e.g., Svalbard is >76°30′N), optical satellite sensors have a limited annual window because of the prolonged polar night, whereas low sun angles and persistent cloud cover reduce data quality during the summer season (Myers-Smith et al., 2020).

The weaker and/or heterogeneous greening response of High Arctic vegetation to warmer air temperatures in the last few decades might thus reflect one or more of the following:

i. Biological limitations: insufficient biomass or plant diversity (including sparse vegetation cover; e.g., Bhatt et al., 2021; Walker et al., 2005).
ii. Abiotic limitations: higher temperatures may not benefit high arctic plant growth (e.g., Marchand et al., 2005) or other abiotic variables may affect observed vegetation patterns (e.g., insufficient soil development, high cryoturbation; Farquharson et al., 2019).
iii. Vegetation index limitations: inability of current reflectance indices and/or sensors to capture ongoing vegetation responses, including inherent limitations due to high cloudiness and low light incident angles (e.g., Berner et al., 2020; Myers-Smith et al., 2015).

Teasing apart between the above limitations in the High Arctic requires comprehensive land cover data to focus on areas with enough vegetation cover, sufficient ground observations of both vegetation and climate, and remote sensing products that provide temporally long, spatially comprehensive records at a fine enough grain to capture some of the high spatial heterogeneity found in High Arctic vegetation. Besides ground-truthing with in situ observations, addressing potential vegetation index limitations may involve extensive cloud detection and even the elaboration of new indices –through new combinations of reflectance bands or novel combinations of the existing indices– that better reflect on-the-ground vegetation. As one of the warmest and fastest warming High Arctic lands, relatively data rich given its latitude, the Svalbard archipelago represents a unique opportunity to comprehensively examine the Greening of the High Arctic tundra.

Here, we used a new cloud-free spatiotemporal dataset from the MODIS Collection 6 data with 232 m pixel resolution interpolated to daily data for Svalbard (Karlsen et al., 2022) to map annual vegetation productivity in terms of OP NDVI –the integrated NDVI from the phenologically-based onset (O) to the Peak (P) of the growth season (Karlsen et al., 2018)– for the entire Svalbard archipelago for the 2000–2022 period. We demonstrate that OP NDVI *i)* is a good proxy for aboveground vegetation productivity and *ii)* shows very high and sustained correlations with temperature data from meteorological stations, and report on an unprecedented recent increase in plant productivity for the archipelago, linked to large and recent changes in the regional climate (Norwegian Centre for Climate Services, n.d.) likely associated with sea ice dynamics.

2. Material and methods

2.1. Study area

The Svalbard archipelago covers about 62,000 km^2 and includes the large islands of Spitsbergen, Nordaustlandet, Edgeøya, and Barentsøya (Fig. 1). The archipelago is located between 76°30′–80°50′N and 10°30′–34°45′E; the isolated, southernmost island Bjørnøya is not included within the present study area. Svalbard is characterized by rugged mountain ranges and glaciers cover more than half of the land surface. The meteorological station Svalbard Lufthavn, close to the administration centre Longyearbyen (Fig. 1), had a mean July air temperature of 7.4 °C during the period 2000–2022 (Norwegian Centre for Climate Services, n.d.). Temperature has increased for all months during the 2000–2022 period. For July, a linear trend shows a temperature increase of 0.08 °C per year, corresponding to 1.74 °C for the 23-year period. The years 2020 and 2022 had the warmest July temperatures in the period with 9.8 °C and 9.3 °C, respectively (the year 2023 had a record high 10.1 °C in July, but it is not included in the study). Annual

mean temperature has increased even more, with a temperature increase of 0.10 °C per year, or 2.55 °C for the whole period.

The largest ice-free areas with vegetation are found on Nordenskiöld Land, a peninsula located in central parts of Spitsbergen characterized by large valleys with dense vegetation cover (Johansen et al., 2012) shown by late July NDVI values >0.5 (Fig. 1). The central parts of Nordenskiöld Land belong in the middle arctic tundra zone, characterized by low shrubs of *Cassiope tetragona* in zonal sites, whereas more peripheral areas are in the colder northern arctic tundra zone with the prostrate dwarf shrub *Dryas octopetala* as a characteristic species (Elvebakk, 2005). Vegetation cover is lower in this latter bioclimatic zone, with a notable exception for manured moss tundra below bird cliffs. Considerable lowland areas have low vegetation cover due to substrate instability, whereas the coldest areas at high altitudes and in the northeast and the east of the archipelago are situated in the cold arctic polar desert zone and have very low vegetation cover. Both the northern Arctic tundra and arctic polar desert categories generally have late July NDVI values below 0.2 (Fig. 1). An exception is areas mapped in the east of Svalbard as manured polar deserts by Elvebakk (2005). These are dominated by *Tomenthypnum nitens* moss tundras in areas

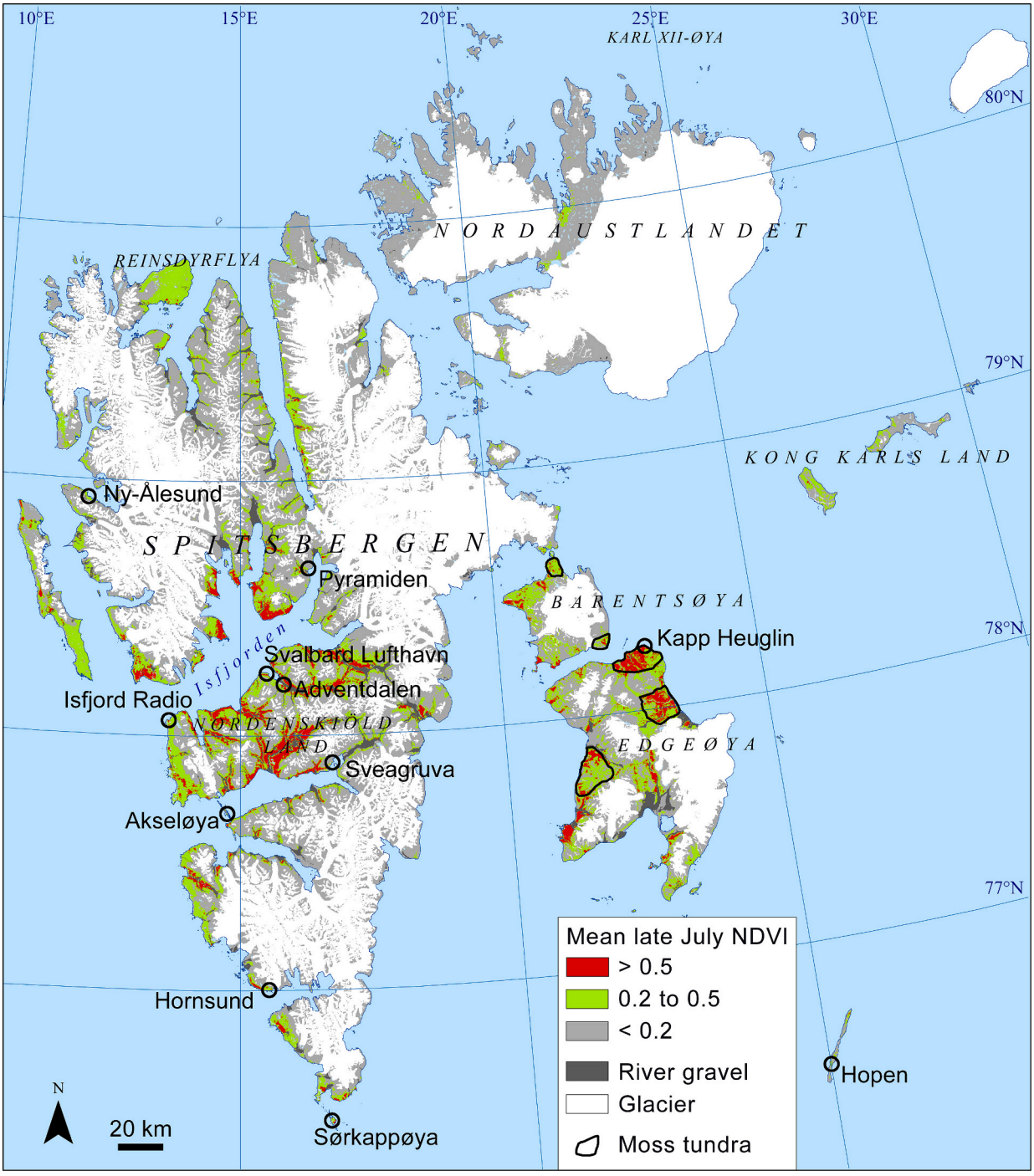

Fig. 1. The study area of Svalbard, showing mean NDVI values for the period 25 July to 1 August, termed late July NDVI, during the 23-year period 2000–2022. Late July is the period with generally high NDVI values for the entire archipelago. Late July NDVI values >0.5 indicate dense vegetation cover and include some manured moss tundra. Late July NDVI values <0.2 indicate no or only scattered vegetation cover and are not included in this study. Positions of the meteorological stations used in this study are indicated by 6 km circles. Areas with discontinuous manured moss tundra within the polar desert zone are redrawn after Elvebakk (2005).

heavily grazed by reindeer. Whereas recent decadal warming has changed dramatically the temperature regimes reported for these bioclimatic units (e.g., Elvebakk and Karlsen, 2022), temperature response in high arctic vegetation is expected to be very slow (Kapfer and Grytnes, 2017; Prach et al., 2010).

2.2. Processing MODIS data

Clear-sky NDVI-maps with 232 m resolution were previously processed for the 2000–2020 period for the entire Svalbard area by (Karlsen et al., 2022), and in the present study the dataset is expanded to include the years 2021 and 2022 (Karlsen, 2023). Two MODIS Terra products, both with 8-day temporal composites, were used. The MOD09A1.V006 product with surface reflectance values for bands 1–7 at 463 m pixel resolution were used to extract information about cloud cover, and the MOD09Q1.V006 product with surface values for bands 1 and 2 at 232 m pixel resolution were used to calculate NDVI values. We use version V006 of MODIS data because the entire time series of MODIS version V061 was not available when the study was carried out. Extensive cloud removal, which includes visual inspection, was done to ensure that most of the noise in the datasets is removed and that most of the noise-free data are retained (see details in Karlsen et al., 2014, 2022). After the process of cloud removal, the dataset was temporally interpolated to daily data as follows: for each 8-day period, the acquisition day of each pixel is known, and this information was used in gap filling of the cloud-free data to daily data. The gap-filling to daily data was achieved by performing Kernel Ridge Regression machine learning method (Camps-Valls et al., 2012), and then smoothed with a Savitzky–Golay filter (5 in windows size and 1 iterations), using the Decomposition and Analysis of Time Series Software (DATimeS) (Belda et al., 2020). The resulting dataset is daily clear-sky NDVI-maps with a 232 m resolution.

2.3. Plant productivity - integrated NDVI from the onset to the peak of the growth season

Previously, the clear-sky MODIS NDVI dataset had been used to map the onset of growth for the 2000–2020 period by (Karlsen et al., 2022), who used time-lapse cameras (phenocams) to record phenophases in field across several vegetation types, as explained by (Karlsen et al., 2021). For dwarf-shrubs, the phenophase named ">5 leaves unfolded, but not yet full size", and for graminoids the phenophase named ">5 leaves (>3 cm) clearly visible" were identified in the time-lapse images (both phenophases have code 15 in Meier, 2018). This phenological stage is defined as 'onset of growth' in the present study (O). It happens rapidly and is easily observed in the field on Svalbard. This stage was first mapped with Sentinel-2 data for central parts of Svalbard for the years 2016–2019 (Karlsen et al., 2021), and Sentinel-2 data were then used to independently evaluate MODIS-NDVI based mapping. The MODIS based onset of growth at each pixel each year was defined as the time when the NDVI value each year exceeded 63 % of the 10 July to 5 August 21-year (2000–2020) mean NDVI value (Karlsen et al., 2022).

In addition, the date of peak NDVI values each year was calculated from the 'raw' unprocessed MOD09Q1.V006 product as follows: we used a pixel-specified average 2000–2022 date of peak NDVI for each pixel instead of yearly date of peak NDVI. A pixel-based timing of peak NDVI accounts for different peak NDVI times in different vegetation types (Anderson et al., 2016; van der Wal and Stien, 2014). A fixed per-pixel average date of peak NDVI was deemed to be more accurate than a yearly date for various reasons. First, Svalbard has a maritime climate with frequent cloud cover. During some years and in some areas, measured maximum NDVI in MODIS data may be to low due to clouds during peak NDVI time, and thereby the measured timing of maximum NDVI will also be inaccurate. Second, field-based hyperspectral FLoX instrument measurements of NDVI close to Longyearbyen (Tømmervik et al., 2023) for the three-year period 2019–2021 show much higher NDVI values in 2020 compared with the two other years, but a remarkably consistent timing of peak NDVI (c. 8 August in a graminoid (*Dupontia fisheri*, *Eriophorum scheuchzeri*) dominated vegetation type), indicating low variability in timing of peak NDVI between years. Finally, the integrated NDVI value from the onset (O) of the growth season each year to the time of average (2000–2022) peak (P) NDVI, hereafter referred to as OP NDVI, was calculated for each vegetated pixel (>0.2 late July NDVI values).

2.4. Relationships between MODIS-NDVI data and temperature data

Eleven meteorological stations on Svalbard have five or more years of daily mean temperature data during the 2000–2022 period (Norwegian Centre for Climate Services, n.d.) in combination with a reasonable vegetation cover as calculated by late July NDVI >0.2 in their surroundings, and were used in this study (Fig. 1). Station SN99760 Sveagruva has incomplete temperature data for the years 2017 and 2018 and for these two years data from the nearby station SN99762 Sveagruva II were instead used.

To link the NDVI data with temperature data from the meteorological stations, a mask with a diameter of 6 km surrounding each station was used (Fig. 1), and only NDVI values from the vegetated areas (defined as late July NDVI >0.2, Fig. 1) within the circle were used. For each meteorological station, OP NDVI, mean July NDVI and integrated NDVI values form 15 July to 15 August (average for the respective mask each year) were calculated, and the temperature for the corresponding periods was calculated. Then, NDVI and temperature parameters were correlated with each other. In addition, annual peak NDVI was compared with mean June–July and mean July temperatures. Since we can assume that the period from onset to peak of growth (OP) corresponds well with the elongation growth of plants and thereby most of the annual aboveground production of vascular plants, the accumulated temperature sum (temperature sum >0 °C) for this period is termed total growing degree days (GDD) and measured as °C-days.

2.5. Greening trend

Estimating linear trends with spatially comprehensive remote sensing data is fraught with difficulties given the large number of pixel-based timeseries involved, which demand large computing power and show large spatial autocorrelation. Moreover, remote sensing timeseries are very often temporally autocorrelated. To account for both spatial and temporal autocorrelation in the estimation of pixel-based linear trends in OP NDVI, we employed the Partitioned Autoregressive Time Series (PARTS) method, developed by (Ives et al., 2021) for analysing spatially autocorrelated time series and available in R as the package *remotePARTS* (R version 4.4.0). In PARTS, the temporal trends in OP NDVI are estimated for each pixel $\boldsymbol{i}$ and represented by coefficient $\boldsymbol{\beta}$ in the regression model:

$$Y_i = a + \beta \times t + \varepsilon_i(t) \quad (1)$$

where random errors $\varepsilon_i(t)$ follow a first order *(t-1)* autoregressive process (AR1; Ives et al., 2021). At the pixel level and for each time series, AR1 models estimate coefficients using restricted maximum likelihood. The temporal trends ($\boldsymbol{\beta}$) are scaled according to the mean OP NDVI for each pixel $\boldsymbol{i}$ to obtain estimates of proportional change. Once the trends have been estimated accounting for first-order autocorrelation, an exponential spatial covariance function ($\boldsymbol{V}$) is used to estimate the expected correlation between their random errors based on their distances ($\boldsymbol{D}$):

$$V = exp\left(\frac{-D}{r}\right) \quad (2)$$

where $\boldsymbol{r}$ is a parameter that dictates the range of spatial autocorrelation (i.e., the distance at which spatial autocorrelation levels out). A nugget ($\boldsymbol{\eta}$) is also estimated, which represents local variation in $\boldsymbol{V}$ that is not

spatially autocorrelated. This can emerge from measurement errors or from small-scale, non-spatially correlated processes that generate local variation in the estimated temporal trends. Both range (***r***) and the nugget (***η***) parameters are estimated from the residuals of the pixel-level time-series models. PARTS allows testing spatial hypotheses through a generalized least-squares regression model (GLS). Here, we used PARTS to test whether there was a trend in OP NDVI values in the study area for the period 2000–2022. To do this, we regressed the temporal coefficients (***β***) on an intercept-only GLS model and assessed the statistical significance of the intercept with a *t-test*. Finally, and given the very large dataset employed in this study, analyses were done through the partitioning all the study area into randomly selected 1500-pixel subsets (totalling 221 subsets) and combining the results from the partitions into an overall statistical test (see Ives et al. (2021) for further details on this method).

2.6. Greening trend and sea-ice

Whereas the western part of the Svalbard archipelago is mostly ice-free due to the warm west Spitsbergen Current, its eastern part is sea-ice covered in winter and has late sea-ice break up some years, which highly influences the tundra productivity due to sea breeze (cold air advection from ice-covered ocean onto adjacent land during the growing season; Macias-Fauria et al., 2017). The Ice Service of the Norwegian Meteorological Institute provides daily sea-ice maps surrounding Svalbard. These maps show both fast ice and different categories of drift ice, where very close drift ice represent 95 % sea-ice cover, close drift ice 80 % cover, open drift ice 55 % cover, and very open drift ice 25 % cover. For each day, we calculated the total area of sea-ice cover east of Svalbard, and then the average for the entire 15 May to 15 September period.

During the study period, sea-ice cover in Svalbard has declined, most notably encompassing the transition from extensive to sparse warm season (15 May to 15 September) sea-ice cover in eastern Svalbard. To explore if the last year with high average cover of sea-ice east of Svalbard represents a structural break in the general 2000–2022 greening trend, we calculated linear trends of OP NDVI before and after the last extensive summer sea-ice year and applied the Chow test (Chow, 1960).

3. Results

3.1. Onset of growth and time of maximum NDVI

Onset of growth each year and average (2000–2022) timing of peak NDVI are used in calculating OP NDVI. Time of onset of growth for the years 2000 to 2020 is shown in (Karlsen et al., 2022) and the years 2021 and 2022 in Fig. S1. In 2021, the onset of growth was 7 days earlier than the 2000–2022 average for the entire Svalbard. The year 2022 had very early onset of growth, with 13 days earlier than the 23-year average, and only the year 2018 had and earlier onset of growth. Overall, the linear trends for the whole period 2000–2022 show generalized earlier onset of the growing season over vegetated areas of Svalbard, with onset starting 1–2 weeks earlier at present than during the early part of the record (Fig. S2).

Early timing of average (2000–2022) peak NDVI, before 25 July, is found in 9.4 % of the mapped areas and is mainly located in parts of the main valley on Nordenskiöld Land (Fig. S3a). Late timings of maximum NDVI, after 14 August, are found on parts of the eastern islands Edgeøya and Barentsøya, and on Reinsdyrflya in the north. Moss tundra lack senescence, and the late peak NDVI areas correspond with the distribution of the moss tundra on the Edgeøya and Barentsøya (Elvebakk, 2005, Fig. 1, Fig. S3a). The number of days with plant elongation growth is defined here as the number of days from the onset of growth (O) each year to the average (2000–2022) timing of peak NDVI (P, Fig. S3b). On average (2000–2022), the growth period lasts between 25 and 30 days in 45 % of the mapped area (Fig. S3b). Growth periods shorter than 25 days are found in some higher areas. Long growth periods (>35 days) are found at some spots on the Edgeøya and Barntsøya islands (Fig. S3b), partly corresponding with the late timing of peak NDVI (Fig. S3a).

3.2. Relationships between temperatures and NDVI

Table 1 shows the relationship between different NDVI variables and temperatures at the 11 meteorological stations used. OP NDVI shows very high and significant correlations with GDD, which is the temperature sum for the same period as OP NDVI. The second-best correlation, but far lower than OP NDVI vs. GDD, is time integrated NDVI (TI NDVI) from 15 June to 15 August correlated with temperatures for the corresponding period, where six of the 11 stations have significant ($p < 0.05$) correlations. Integrated NDVI for July vs. July temperature correlates significantly ($p < 0.05$) for five of the 11 stations. Maximum NDVI does not correlate well either with mean July or with mean June–July temperatures. This shows that OP NDVI by far best reflects the temperature regimes and therefore also the corresponding vegetation growth patterns.

While Table 1 shows the OP NDVI–GDD correlation for each station, Fig. 2 shows that there is also a strong general linear relationship ($r^2 = 0.590$, $p = 1.95e\text{-}31$, $n = 155$). The OP NDVI increased by 4.00 for each 100 °C-days increase in GDD (Fig. 2). The meteorological station Kapp Heuglin on Edgeøya island is in an area with moss-tundra and is an outlier in the general correlation. Without the Kapp Heuglin station the general correlation between OP NDVI and GDD increases to $r^2 = 0.698$. From the Kapp Heuglin station data alone, OP NDVI values increase by 7.79 for each 100 °C-days increase in growing degree days, indicating a different temperature–NDVI relationship in moss-tundra compared with areas with a field layer of vascular plants. A linear model accounting for interactions between GDD and Station (OP NDVI ~ GDD + Station + GDD * Station) resulted in significant coefficients for GDD (p-value = 2.12e-06) and for the interaction GDD * Kapp Heuglin (p-value = 0.010), indicating a statistically significant difference in the slope parameter when controlled for the different meteorological stations (Table S1). An interaction analysis between factor (Station) and covariate (GDD; computed in R using the emmeans package, v.1.10.0) further confirmed the outlier nature of Kapp Heuglin, which was the only meteorological station for which the model showed statistically significant differences when compared pairwise with the other stations ($p < 0.05$ in 7 out of 10 possible pairwise comparisons and displaying a higher slope in all cases; Table S2 and Fig. S4). In the pairwise comparisons, p-values were adjusted using the Tukey method (or Tukey's honestly significant difference test).

3.3. Variability and trends in OP NDVI

High average (2000–2022) OP NDVI values and thereby high plant productivity, defined here as above 12.5 units (corresponding to a GDD of 297 °C-days based on Fig. 2), are mainly found at the lower elevations of the main valleys of Nordenskiöld Land and in some areas on the north side of Isfjorden (Fig. 3), both areas being among the warmest in Svalbard (Elvebakk, 2005). OP NDVI values below 5 (< 109 °C-days) are found at higher elevations in central parts of Svalbard, on Reindsdyrflya in the north, and on the polar desert islands Hopen and Kong Karls Land.

Looking at regional averages of OP NDVI, the years 2000 and 2008 were extreme in terms of low OP NDVI values (Fig. 4), and during those years 78 % and 88 %, respectively, of the mapped area shows OP NDVI values of at least 2 units below the 2000–2022 average (Fig. S3). Those years also had the highest average cover of sea-ice (> 42 %) east of Svalbard in the 15 May to 15 September period (see the definition of the area and the sea ice extent timeseries in Fig. S6), and there is a significant negative correlation between the sea ice extent and OP NDVI values (Fig. S7). The most extreme year in terms of high OP NDVI values is 2022. During this year, 91 % of the mapped area had OP NDVI values of >2 units above the 23-year average. In the year 2008, the average OP NDVI values for the all the vegetated area (late July NDVI >0.20) was

Table 1
Correlation (r^2) values between NDVI and temperature parameters from 11 meteorological stations. *** $p < 0.001$, **$p < 0.01$, *$p < 0.05$. Number of years with temperature data shown in brackets.

Meteorological stations	OP NDVI/ GDD	July NDVI/July temperature	15 June–15 Aug. NDVI/15 June–15 Aug. temperature	Max. NDVI/July temperature	Max. NDVI/June–July temperature
99720 Hopen	0.872***(23)	0.419*** (23)	0.426*** (23)	0.271* (23)	0.222* (23)
99735 Kapp Heuglin	0.878*** (15)	0.493** (11)	0.753*** (11)	0.400* (14)	0.402* (11)
99752 Sørkappøya	0.847** (7)	0.633 (15)	0.462 (3)	0.028 (5)	0.348 (4)
99754 Hornsund	0.907*** (13)	0.712*** (13)	0.636** (10)	0.620** (13)	0.670* (8)
99760 Sveagruva	0.870*** (17)	0.117 (18)	0.048 (17)	0.024 (16)	0.056 (16)
99765 Akseløya	0.785*** (11)	0.065 (11)	0.283 (9)	0.001 (11)	0.004 (11)
99790 Isfjord Radio	0.837*** (12)	0.440** (13)	0.479* (11)	0.033 (13)	0.014 (11)
99840 Svalbard Lufthavn	0.849*** (22)	0.585*** (22)	0.682*** (21)	0.131 (22)	0.067 (21)
99870 Adventdalen	0.789* (6)	0.002 (6)	0.144 (6)	0.660* (6)	0.579(6)
99880 Pyramiden	0.862*** (8)	0.007 (5)	0.007 (5)	0.165 (7)	0.082 (7)
99910 Ny-Ålesund	0.879*** (21)	0.276 (22)	0.453*** (21)	0.056 (22)	0.092 (19)

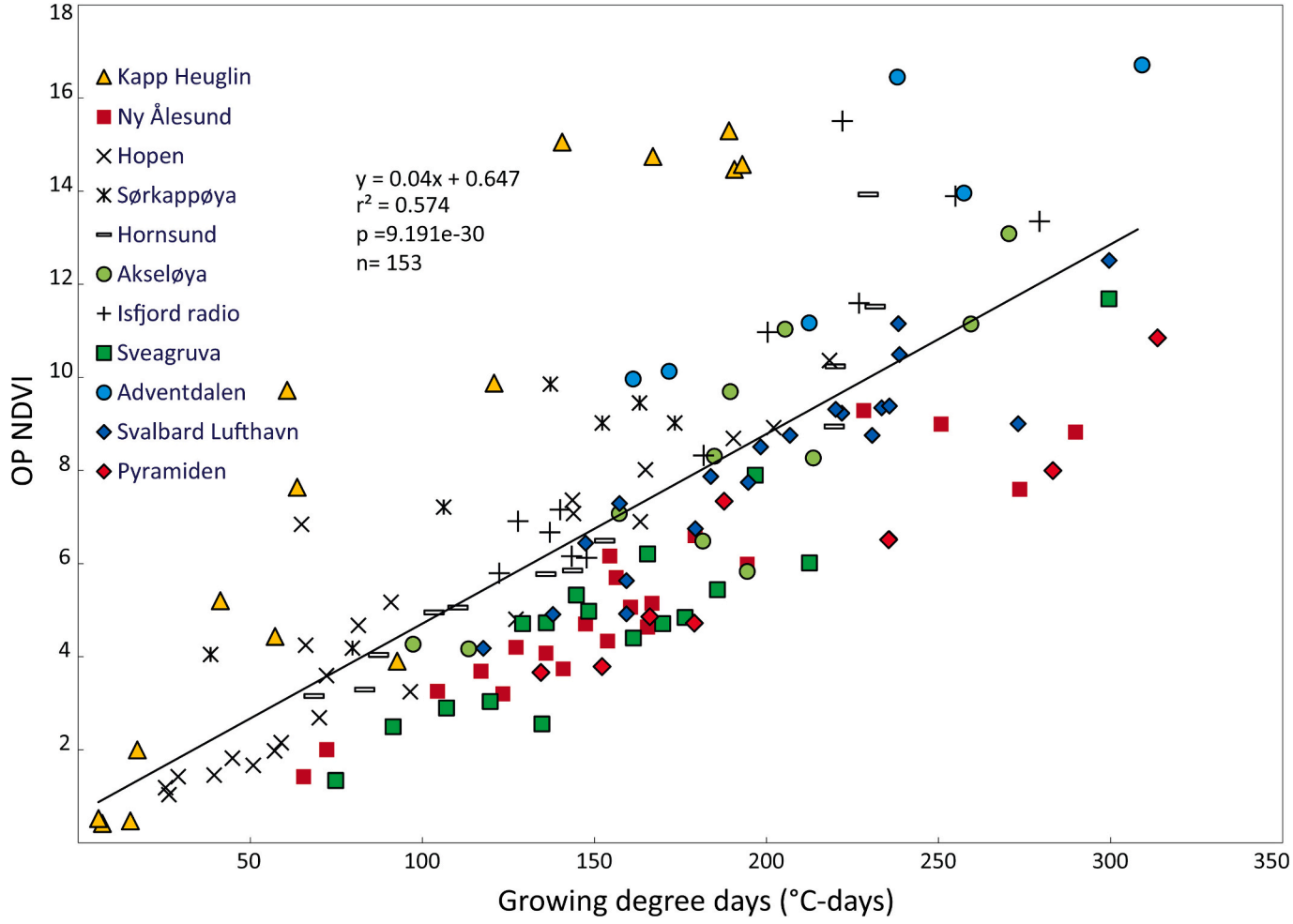

Fig. 2. Relationship between OP NDVI values and corresponding GDD.

2.33, compared to 12.32 in 2022 (Fig. 4). The four years with the highest average tundra productivity (mean OP NDVI values for all vegetated areas) are all found recently, from 9.09 OP NDVI units in 2016, to 9.98 in 2018, 11.58 in 2020 and 12.32 in 2022 (Fig. 4).

If we only look at areas with dense vegetation (late July NDVI >0.50, Fig. 1) the trend is even stronger (Fig. 4). In 2008 the average cover of sea-ice east of Svalbard in the 15 May to 15 September period was 43 %. All years after 2008 had less cover of sea-ice in the same period (Fig. S4). In the OP NDVI time-series, the year 2008 can significantly be identified ($p = 0.022$, chow statistics = 4.730 for mean late July NDVI >0.5 and p

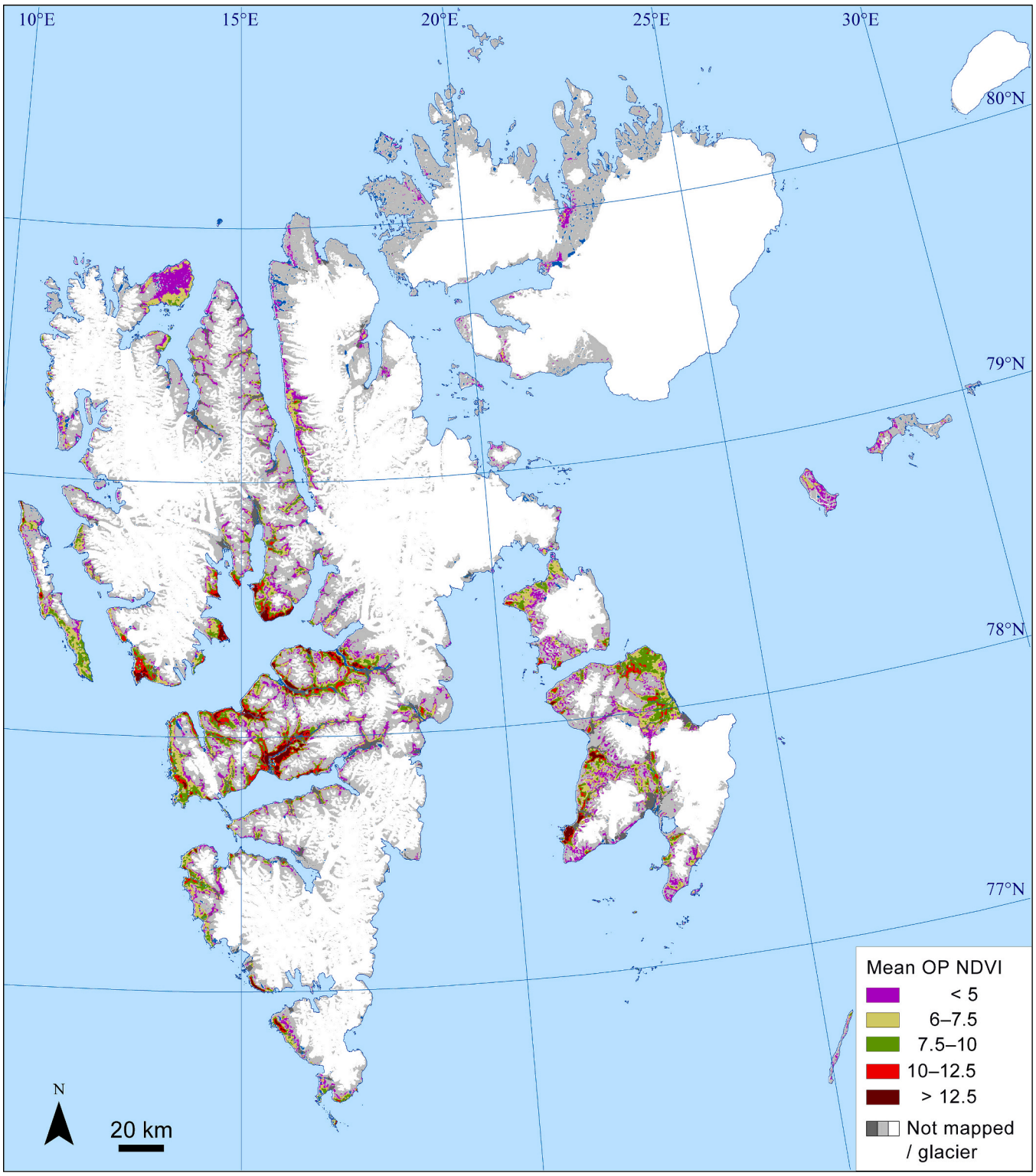

Fig. 3. Mean (2000–2022) OP NDVI values.

= 0.017, chow statistics = 5.192 for mean late July NDVI >0.2) as a breaking point. The period 2000 to 2008 has a weak decreasing non-significant trend in vegetation productivity, while the 2000–2022 period has a strong significant increase. The increasing trend from 2008 to 2022 is 0.648 OP NDVI units yr^{-1} for the areas with dense vegetation cover, which is a rate double than that of the whole 2000–2022 period (0.326 OP NDVI units yr^{-1}).

The GLS model further confirmed that OP NDVI values showed a statistically significant positive trend in the study area for the period 2000–2022, even when accounting for temporal and spatial autocorrelation (t-statistic 4.087, p-value <0.0001).

Fig. 5a shows the 23-year linear trend in OP NDVI, run on a regression with temporal autocorrelation. On average for the entire archipelago, the trend is 5.04 OP NDVI units (0.219 yr^{-1}) for 2000 to 2022 (Fig. 4), which corresponds to an increase of 126 °C-days. However, there are regional differences (Fig. 5a). The highest increase is found in

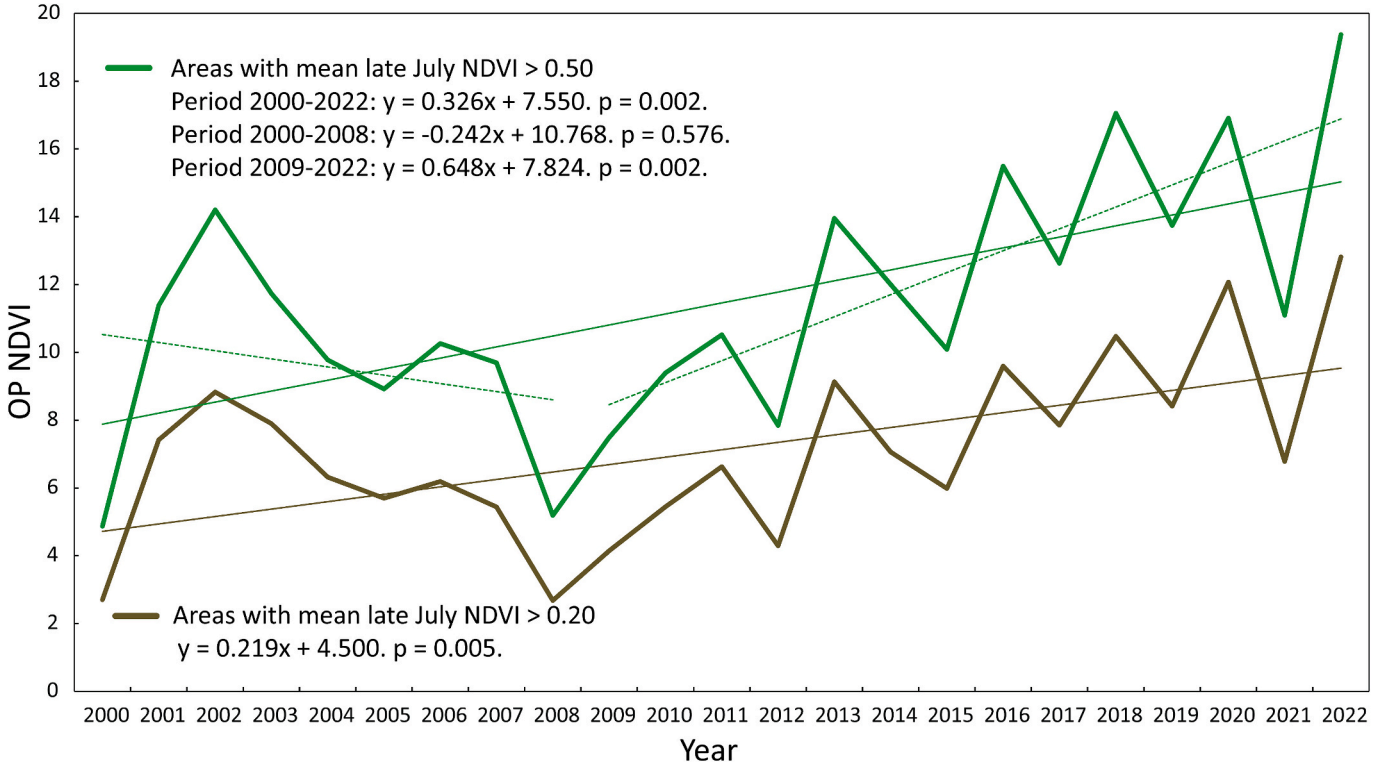

Fig. 4. Mean annual OP NDVI values for the entire Svalbard archipelago, for all the vegetated areas (mean late July NDVI >0.20), and for the most densely vegetated areas (mean late July NDVI >0.50).

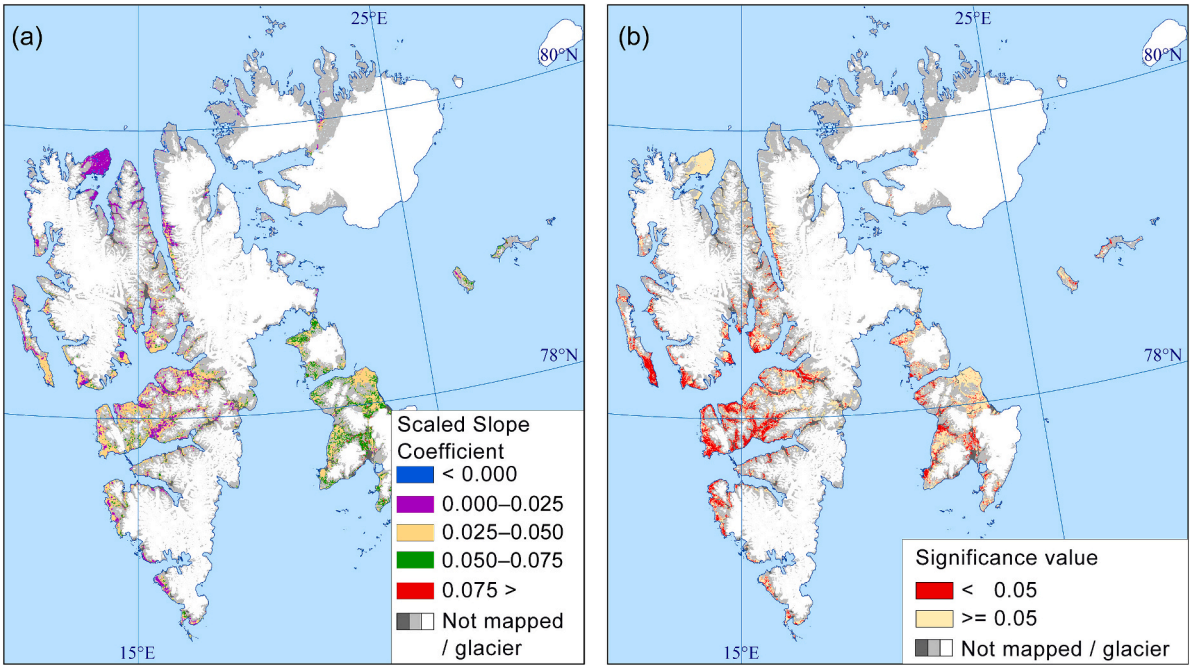

Fig. 5. Patterns of temporal trends in OP NDVI, 2000–2022. (a) Temporal trends in NDVI measured by the slope coefficient value from regression with auto-correlated errors scaled by the mean OP NDVI in each pixel (i.e., trend proportional to the OP NDVI mean for each pixel). (b) Pixels for which the linear trend is significant ($p < 0.05$).

Nordenskiöld Land, the north side of Isfjorden, and in some parts of Edgeøya and Kong Karls Land. Most of these increases in OP NDVI values are significant ($p < 0.05$, Fig. 5b). Only a small increase in OP NDVI is found on Reinsdyrflya in the north. Adventdalen valley, close to the Svalbard administration centre Longyearbyen, also shows a statistically significant increase in parts, with an average increase of about 5 OP NDVI units (108 °C-days). When using 2008 as a breaking point in the time-series and analyses, the increasing trend for the 2008–2022 period is steep and significant ($p < 0.05$) in 60 % of the mapped area (Fig. 4, Fig. S8), and the highest increase (>10 OP NDVI units) is found in most

of Edgeøya and Kong Karls Land. Notably, Reinsdyrflya in the north does show large areas with pixels featuring a statistically significant greening trend for this later sub-period (Fig. S8b). Overall, the GLS model for the region and sub-period 2008–2022 confirms a statistically significant regionally increase in OP NDVI, even more so than for the full period, in agreement with the regional averages (t-statistic 7.795, p-value = 6.480e-15).

4. Discussion

4.1. NDVI – temperature relationship

High and significant correlations between OP NDVI and GDD have been found, both for each meteorological station and as a general relationship using temperatures from all stations (Table 1, Fig. 2). It is well known that NDVI correlates with temperatures in arctic areas, however, this study demonstrates much higher temperature–NDVI correlations than in any other study known to us. And that no weakening relationship between NDVI and temperatures for the 2000–2022 period is found in this study. Most other studies use maximum NDVI or NDVI values integrated over two to three summer months or during the photosynthetically active period, e.g., (Beck and Goetz, 2011; U. Bhatt et al., 2013; Park et al., 2016; Xu et al., 2013). In our study, such more commonly applied NDVI parameters provide a rather poor, and often non-significant fit with temperatures, thereby demonstrating the superiority of OP NDVI. Maximum NDVI in particular provides poor correlation with temperature data, which may be explained by the maritime climate on Svalbard with frequent cloud cover: during some years and in some areas, measured maximum NDVI may be too low due to clouds during peak NDVI time.

4.2. NDVI – biomass relationship

NDVI is widely used to measure vegetation productivity (Kooistra et al., 2024), and it is reasonable to believe that our OP NDVI values reflect vegetation productivity very well. A previous study (Karlsen et al., 2018) found a significant correlation between MODIS based OP NDVI values and field measurements of plant production at Nordenskiöld Land in central parts of Svalbard. The field data mainly consist of the annual growth of vascular plants, also including a small amount of perennial above-ground biomass. Unfortunately, the field data in Karlsen et al. (2018) were not designed for upscaling with MODIS data. Karlsen et al. (2018) were only able to compare field data with MODIS data from the widespread moist *Luzula* heath, and did not use field data from ridges (due to too scattered vegetation given the MODIS 232 m pixel size) nor from marshes (due to too small marsh patches given the MODIS pixel size). Then, they compared field biomass measurements against OP NDVI values for two different masks: a local mask surrounding the field with moist *Luzula* heath data and a regional mask of parts of central Svalbard (405 km^2) of vegetated areas. For the earlier they found that productivity (g m^{-2}) = 1.70 * OP NDVI +6.01, with an adjusted $r^2 = 0.51$ ($p = 0.01$). for the latter, they found that productivity (g m^{-2}) = 1.42 * OP NDVI +10.2, with an adjusted $r^2 = 0.44$ ($p = 0.02$). These results indicate that 10 OP NDVI units represent 14.2 to 17.0 g m^{-2} of vascular plant dry biomass, depending on the relationship used. In the present study, we used the Collection 6 of MODIS data, as compared with the previous Collection 5 by Karlsen et al. (2018) and used an interpolation/smoothing method which lowers the NDVI values (1 in iterations in the Savitzky–Golay filter). Hence, an increase of 10 OP NDVI units in the present study should indicate an increase in plant productivity higher than the 14.2 to 17.0 g m^{-2} reported in Karlsen et al. (2018).

Assuming that 10 OP NDVI units correspond to 14.2 to 17.0 g m^{-2}, our results would indicate an increase in vegetation production of 97,236 to 116,410 t of dry weight (which includes some perennial biomass) in the 6848 km^2 of Svalbard with vegetation cover (defined as late July NDVI >0.20, Fig. 1) covered in this study for the growing season of 2022 as compared to 2008. While these numbers are highly uncertain since the relationships were taken from only a portion of Svalbard and a limited number of land cover types, we believe they might be accurate to at least the same order of magnitude. However, there is an obvious need for extensive field validation data designed to be upscaled to MODIS data with productivity estimates in g m^{-2} across major vegetation types in order to establish a more reliable OP NDVI – vegetation productivity relationship, as recommended by Karlsen et al. (2019) and shown by Stendardi (2020). A limitation in the present study is the inclusion of stable tundra vegetation only with summer NDVI >0.2, as the method applied relies on certain dynamics in NDVI values during the growing season. Areas with summer NDVI <0.2 cover large areas in Svalbard and are either unstable areas or polar deserts, which also have vegetation, although with low cover. Another major challenge of the present study is the interpretation of the results in areas dominated by moss-tundra.

4.3. Moss-tundra

The relationship between OP NDVI and GDD at the meteorological station Kapp Heuglin on eastern Edgeøya island is a clear outlier in the general OP NDVI – GDD relationship (Fig. 2, Fig. S4, Tables S1 & S2): whereas it is very high and significant (Table 1, $r^2 = 0.812$, $p = 2.59E-07$, $n = 12$), OP NDVI increases by 7.79 for each 100 °C-days increase, compared with OP NDVI increases of 4.00 for each 100 °C-days increase as a mean value for all the meteorological stations. Indeed, the difference in the slope of this relationship when accounting for the station Kapp Heuglin is significantly different to that of all other meteorological stations. The meteorological station Kapp Heuglin is situated within the polar desert zone, with discontinuous manured moss-tundra (Elvebakk, 2005). Characteristic for Svalbard is its widespread moss-tundra dominated by *Tomentypnum nitens*, which produces moss carpets with a thin active layer and accumulates thick peat layers without a standing water level (Vanderpuye et al., 2002). Such luxuriant moss carpet formation occurs in very cold environments and depends on nutrients from sea bird colonies or from intensive reindeer grazing and is absent from arctic areas with large rodent populations. Bryophytes are evergreen and they do not share the greening phenological cycle of most vascular plant species. The *Tomenthypnum* carpets are maintained by a high permafrost level and are developed primarily by the humidity of a thin active layer and by manuring. Onset of growth could be mapped very early in bryophyte-dominated areas with the method used in this study, as previous studies have shown (Karlsen et al., 2021, 2022), and such areas may attain their highest NDVI value very late in the season due to lack of a clear senescence reflectance signal and that moss biomass increases throughout the season as moss growth is less limited by temperatures (Arndal et al., 2009, Fig. S3a). This results in a much longer measured period spanning the onset to the average timing of maximum of growth (OP NDVI) in moss-tundra (Fig. S3b) as compared with areas with a field layer of vascular plants, which might partly explain the higher slope relating OP NDVI and GDD in areas dominated by these bryophyte communities. Besides, the manured moss-tundra in the polar desert zone has both high biomass (Elvebakk, 2005) and high moisture content. The latter also contributes to a high NDVI value, since high moisture lowers the reflectance value in the red band more than in the NIR band (May et al., 2018). This strongly suggests that there is a need for a separate method to measure vegetation productivity in moss-tundra, and that our results for these areas cannot be readily compared to those of other tundra ecosystems which are the primary targets of this study. If applying the OP NDVI method in other high arctic areas, the challenge with the moss-tundra will probably be reduced. The polar desert moss-tundra appears to be restricted to Svalbard and, probably, neighboring Novaya Zemlya. This may be due to the absence of rodents and the high seabird density, which is related to the mild sea currents reaching further to the north here and which implies manuring of surrounding

ecosystems (Vanderpuye et al., 2002). In the present study, extensive cloud screening of the imagery, including visual inspection, was done to ensure that most of the noise in the datasets is removed and that most of the noise-free data are retained. Our OP NDVI method also requires mapping the onset of growth, as validated from field phenology data in our study. This limits the possibility to apply the method on a circumpolar scale. If our OP NDVI method is applied to a more continental part of the high arctic with less clouds, then the annual date of maximum NDVI when calculating OP NDVI should be explored, instead of the mean date of maximum NDVI as in this study.

4.4. Temporal dynamics of the Greening of Svalbard – links to sea ice

Annual plant biomass measurements in Nordenskiöld Land between 1998 and 2009 (van der Wal and Stien, 2014), revealed twofold variation (range 23–46 g m^{-2}) between years. The present study concludes that OP NDVI values –an indication of vegetation production– were exceptionally high in 2022, followed by the year 2020, followed by the year 2018 and then followed by the year 2016. These years had all higher productivity compared to any year during the 2000–2015 period (Fig. 4). This shows a rapid recent greening trend, possibly starting in 2008 (Fig. 4). The year 2008 was the last year with high average cover of sea-ice in the 15 May to 15 September period in eastern parts of Svalbard to date. Extensive sea ice close to the coast was shown to reduce NDVI in parts of the archipelago affected by sea ice (Fig. S6, Macias-Fauria et al., 2017). In Svalbard, and according to the OP NDVI trends, plant production of vascular plants was most likely more than twice higher in 2022 compared to years like 2000 and 2008. Our study also uncovers large regional differences (Fig. 5, Figs. S5, S8), with the highest increase in eastern parts (Edgeøya and Barentsøya islands) and less in the north (Reinsdyrflya), which we suggest are likely related to changes in the timing of the break-up of the sea-ice.

5. Conclusion

We demonstrate that a new vegetation index (OP NDVI) rooted in an understanding of High Arctic vegetation phenology reliably retrieves information of on-the-ground vegetation productivity and shows very high, significant, and sustained correlation with temperature data for the corresponding period (growing degree days) on Svalbard. Our index is based on a MODIS dataset where only the cloud-free parts of the images are used and then interpolated to daily data. It is also based on mapping the onset of growth with a clear phenological definition, as interpreted from field-based phenological measurements designed for up-scaling by remote sensing data. Moreover, our study reports for the first time a recent rapid increase in Svalbard tundra productivity (OP NDVI), strongly related to the recent temperature increase during the growth season, and which agrees with the transition from perennial sea ice to absent sea ice around the eastern part of the archipelago. Where moss-tundra dominates, the OP NDVI-based results are uncertain, due to the lack of a clear phenological cycle in the dominating bryophytes. Finally, of the limitations in detecting the greening of the High Arctic listed in the Introduction, our results suggest that when utilising the right vegetation indices at sufficient spatial grain and coverage, the High Arctic archipelago of Svalbard has the biological capacity and is currently responding to increases in air temperature through an increase in aboveground biomass.

CRediT authorship contribution statement

Stein Rune Karlsen: Writing – review & editing, Writing – original draft, Visualization, Validation, Software, Methodology, Investigation, Funding acquisition, Formal analysis, Data curation. **Arve Elvebakk:** Writing – original draft, Validation, Investigation. **Laura Stendardi:** Writing – original draft, Validation, Data curation. **Kjell Arild Høgda:** Writing – original draft, Methodology, Funding acquisition, Data curation. **Marc Macias-Fauria:** Writing – review & editing, Writing – original draft, Validation, Investigation.

Declaration of competing interest

The authors declare the following financial interests/personal relationships which may be considered as potential competing interests: Stein Rune Karlsen reports financial support was provided by Norwegian Space Agency. If there are other authors, they declare that they have no known competing financial interests or personal relationships that could have appeared to influence the work reported in this paper.

Data availability

Data will be made available on request.

Acknowledgements

This study was supported by the Research Council of Norway under the project Svalbard Integrated Arctic Earth Observing System—Infrastructure development of the Norwegian node (SIOS-InfraNor Project No. 269927). This SIOS project (InfraNord instrument #51) is funded by the Norwegian Space Agency (NoSA).

Appendix A. Supplementary data

Supplementary data to this article can be found online at https://doi.org/10.1016/j.scitotenv.2024.174130.

References

Anderson, H.B., Nilsen, L., Tømmervik, H., Karlsen, S.R., Nagai, S., Cooper, E.J., 2016. Using ordinary digital cameras in place of near-infrared sensors to derive vegetation indices for phenology studies of High Arctic vegetation. Remote Sens. 8 (10) https://doi.org/10.3390/rs8100847.

Arndal, M.F., Illeris, L., Michelsen, A., Albert, K., Tamstorf, M., Hansen, B.U., 2009. Seasonal variation in gross ecosystem production, plant biomass, and carbon and nitrogen pools in five High Arctic vegetation types. Arct. Antarct. Alp. Res. 41 (2), 164–173. https://doi.org/10.1657/1938-4246-41.2.164.

Beck, P.S.A., Goetz, S.J., 2011. Satellite observations of high northern latitude vegetation productivity changes between 1982 and 2008: ecological variability and regional differences. Environ. Res. Lett. 6 (4), 045501 https://doi.org/10.1088/1748-9326/6/4/045501.

Belda, S., Pipia, L., Morcillo-Pallarés, P., Rivera-Caicedo, J.P., Amin, E., De Grave, C., Verrelst, J., 2020. DATimeS: A machine learning time series GUI toolbox for gap-filling and vegetation phenology trends detection. Environ. Model. Softw. 127, 104666 https://doi.org/10.1016/j.envsoft.2020.104666.

Berner, L.T., Massey, R., Jantz, P., Forbes, B.C., Macias-Fauria, M., Myers-Smith, I., Kumpula, T., Gauthier, G., Andreu-Hayles, L., Gaglioti, B.V., Burns, P., Zetterberg, P., D'Arrigo, R., Goetz, S.J., 2020. Summer warming explains widespread but not uniform greening in the Arctic tundra biome. Nat. Commun. 11 (1), 4621. https://doi.org/10.1038/s41467-020-18479-5.

Bhatt, U., Walker, D., Raynolds, M., Bieniek, P., Epstein, H., Comiso, J., Pinzon, J., Tucker, C., Polyakov, I., 2013. Recent declines in warming and vegetation greening trends over Pan-Arctic tundra. Remote Sens. 5 (9), 4229–4254. https://doi.org/10.3390/rs5094229.

Bhatt, U.S., Walker, D.A., Raynolds, M.K., Walsh, J.E., Bieniek, P.A., Cai, L., Comiso, J.C., Epstein, H.E., Frost, G.V., Gersten, R., Hendricks, A.S., Pinzon, J.E., Stock, L., Tucker, C.J., 2021. Climate drivers of Arctic tundra variability and change using an indicators framework. Environ. Res. Lett. 16 (5) https://doi.org/10.1088/1748-9326/abe676.

Campbell, T.K.F., Lantz, T.C., Fraser, R.H., Hogan, D., 2021. High Arctic vegetation change mediated by hydrological conditions. Ecosystems 24 (1), 106–121. https://doi.org/10.1007/s10021-020-00506-7.

Camps-Valls, G., Munoz-Mari, J., Gomez-Chova, L., Guanter, L., Calbet, X., 2012. Nonlinear statistical retrieval of atmospheric profiles from MetOp-IASI and MTG-IRS infrared sounding data. IEEE Trans. Geosci. Remote Sens. 50 (5), 1759–1769. https://doi.org/10.1109/TGRS.2011.2168963.

Chow, G.C., 1960. Tests of equality between sets of coefficients in two linear regressions. Econometrica 28 (3), 591–605. https://doi.org/10.2307/1910133.

Edlund, S.A., Alt, B.T., 1989. Regional congruence of vegetation and summer climate patterns in the Queen Elizabeth Islands, Northwest Territories, Canada. Arctic 42 (1), 3–23. http://www.jstor.org/stable/40510768.

Elmendorf, S.C., Henry, G.H.R., Hollister, R.D., Björk, R.G., Boulanger-Lapointe, N., Cooper, E.J., Cornelissen, J.H.C., Day, T.A., Dorrepaal, E., Elumeeva, T.G., Gill, M., Gould, W.A., Harte, J., Hik, D.S., Hofgaard, A., Johnson, D.R., Johnstone, J.F., Jónsdóttir, I.S., Jorgenson, J.C., Wipf, S., 2012. Plot-scale evidence of tundra

vegetation change and links to recent summer warming. Nat. Clim. Chang. 2 (6), 453–457. https://doi.org/10.1038/nclimate1465.
Elvebakk, A., 2005. A vegetation map of Svalbard on the scale 1:3.5 mill. Phytocoenologia 35 (4), 951–967. https://doi.org/10.1127/0340-269X/2005/0035-0951.
Elvebakk, A., Karlsen, S.R., 2022. Det arktiske Finnmark – ein bioklimatisk studie av område nord for den polare skoggrensa. Blyttia 80 (3), 147–174.
Epstein, H.E., Raynolds, M.K., Walker, D.A., Bhatt, U.S., Tucker, C.J., Pinzon, J.E., 2012. Dynamics of aboveground phytomass of the circumpolar Arctic tundra during the past three decades. Environ. Res. Lett. 7 (1), 015506 https://doi.org/10.1088/1748-9326/7/1/015506.
Farquharson, L.M., Romanovsky, V.E., Cable, W.L., Walker, D.A., Kokelj, S.V., Nicolsky, D., 2019. Climate change drives widespread and rapid thermokarst development in very cold permafrost in the Canadian High Arctic. Geophys. Res. Lett. 46 (12), 6681–6689. https://doi.org/10.1029/2019GL082187.
Guay, K.C., Beck, P.S.A., Berner, L.T., Goetz, S.J., Baccini, A., Buermann, W., 2014. Vegetation productivity patterns at high northern latitudes: a multi-sensor satellite data assessment. Glob. Chang. Biol. 20 (10), 3147–3158. https://doi.org/10.1111/gcb.12647.
Isaksen, K., Nordli, Ø., Ivanov, B., Køltzow, M.A.Ø., Aaboe, S., Gjelten, H.M., Mezghani, A., Eastwood, S., Førland, E., Benestad, R.E., Hanssen-Bauer, I., Brækkan, R., Sviashchennikov, P., Demin, V., Revina, A., Karandasheva, T., 2022. Exceptional warming over the Barents area. Sci. Rep. 12 (1) https://doi.org/10.1038/s41598-022-13568-5.
Ives, A.R., Zhu, L., Wang, F., Zhu, J., Morrow, C.J., Radeloff, V.C., 2021. Statistical inference for trends in spatiotemporal data. Remote Sens. Environ. 266 https://doi.org/10.1016/j.rse.2021.112678.
Jeganathan, C., Dash, J., Atkinson, P.M., 2014. Remotely sensed trends in the phenology of northern high latitude terrestrial vegetation, controlling for land cover change and vegetation type. Remote Sens. Environ. 143, 154–170. https://doi.org/10.1016/j.rse.2013.11.020.
Johansen, B.E., Karlsen, S.R., Tømmervik, H., 2012. Vegetation mapping of Svalbard utilising Landsat TM/ETM+ data. Polar Record 48 (1). https://doi.org/10.1017/S0032247411000647.
Kapfer, J., Grytnes, J.A., 2017. Large climate change, large effect? Vegetation changes over the past century in the European high Arctic. Appl. Veg. Sci. 20 (2) https://doi.org/10.1111/avsc.12280.
Karlsen, S.R., 2023. NDVI for Svalbard. https://doi.org/10.21343/30HV-1E14.
Karlsen, S.R., Elvebakk, A., 2003. A method using indicator plants to map local climatic variation in the Kangerlussuaq/Scoresby Sund area, East Greenland. J. Biogeogr. 30 (10), 1469–1491. https://doi.org/10.1046/j.1365-2699.2003.00942.x.
Karlsen, S.R., Elvebakk, A., Høgda, K.A., Grydeland, T., 2014. Spatial and temporal variability in the onset of the growing season on svalbard, arctic Norway - measured by MODIS-NDVI satellite data. Remote Sens. 6 (9) https://doi.org/10.3390/rs6098088.
Karlsen, S.R., Anderson, H.B., Van Der Wal, R., Hansen, B.B., 2018. A new NDVI measure that overcomes data sparsity in cloud-covered regions predicts annual variation in ground-based estimates of high arctic plant productivity. Environ. Res. Lett. 13 (2) https://doi.org/10.1088/1748-9326/aa9f75.
Karlsen, S.R., Stendardi, L., Nilsen, L., Malnes, E., Eklundh, L., Julitta, T., Burkart, A., Tømmervik, H., 2019. Sentinel satellite-based mapping of plant productivity in relation to snow duration and time of green-up (GROWTH). In: SESS Report 2019. The State of Environmental Science in Svalbard – An Annual Report, 9296.
Karlsen, S.R., Stendardi, L., Tømmervik, H., Nilsen, L., Arntzen, I., Cooper, E.J., 2021. Time-series of cloud-free Sentinel-2 NDVI data used in mapping the onset of growth of Central Spitsbergen, Svalbard. Remote Sens. 13 (15) https://doi.org/10.3390/rs13153031.
Karlsen, S.R., Elvebakk, A., Tømmervik, H., Belda, S., Stendardi, L., 2022. Changes in onset of vegetation growth on Svalbard, 2000–2020. Remote Sens. 14 (24), 6346. https://doi.org/10.3390/rs14246346.
Kooistra, L., Berger, K., Brede, B., Graf, L.V., Aasen, H., Roujean, J.-L., Machwitz, M., Schlerf, M., Atzberger, C., Prikaziuk, E., Ganeva, D., Tomelleri, E., Croft, H., Reyes Muñoz, P., Garcia Millan, V., Darvishzadeh, R., Koren, G., Herrmann, I., Rozenstein, O., Verrelst, J., 2024. Reviews and syntheses: remotely sensed optical time series for monitoring vegetation productivity. Biogeosciences 21 (2), 473–511. https://doi.org/10.5194/bg-21-473-2024.
Macias-Fauria, M., Karlsen, S.R., Forbes, B.C., 2017. Disentangling the coupling between sea ice and tundra productivity in Svalbard. Sci. Rep. 7 (1) https://doi.org/10.1038/s41598-017-06218-8.
Marchand, F.L., Mertens, S., Kockelbergh, F., Beyens, L., Nijs, I., 2005. Performance of High Arctic tundra plants improved during but deteriorated after exposure to a simulated extreme temperature event. Glob. Chang. Biol. 11 (12), 2078–2089. https://doi.org/10.1111/j.1365-2486.2005.01046.x.
May, J.L., Parker, T., Unger, S., Oberbauer, S.F., 2018. Short term changes in moisture content drive strong changes in Normalized Difference Vegetation Index and gross primary productivity in four Arctic moss communities. Remote Sens. Environ. 212, 114–120. https://doi.org/10.1016/j.rse.2018.04.041.
Growth stages of mono- and dicotyledonous plants. In: Meier, U. (Ed.), 2018. BBCH Monograph. *Federal Biological Research Centre for Agriculture and Forestry*. https://doi.org/10.5073/20180906-074619.
Myers-Smith, I.H., Elmendorf, S.C., Beck, P.S.A., Wilmking, M., Hallinger, M., Blok, D., Tape, K.D., Rayback, S.A., Macias-Fauria, M., Forbes, B.C., Speed, J.D.M., Boulanger-Lapointe, N., Rixen, C., Lévesque, E., Schmidt, N.M., Baittinger, C., Trant, A.J., Hermanutz, L., Collier, L.S., Vellend, M., 2015. Climate sensitivity of shrub growth across the tundra biome. Nat. Clim. Chang. 5 (9), 887–891. https://doi.org/10.1038/nclimate2697.
Myers-Smith, I.H., Kerby, J.T., Phoenix, G.K., Bjerke, J.W., Epstein, H.E., Assmann, J.J., John, C., Andreu-Hayles, L., Angers-Blondin, S., Beck, P.S.A., Berner, L.T., Bhatt, U.S., Bjorkman, A.D., Blok, D., Bryn, A., Christiansen, C.T., Cornelissen, J.H.C., Cunliffe, A.M., Elmendorf, S.C., Wipf, S., 2020. Complexity revealed in the greening of the Arctic. Nat. Clim. Chang. 10 (2), 106–117. https://doi.org/10.1038/s41558-019-0688-1.
Myneni, R.B., Keeling, C.D., Tucker, C.J., Asrar, G., Nemani, R.R., 1997. Increased plant growth in the northern high latitudes from 1981 to 1991. Nature 386 (6626), 698–702. https://doi.org/10.1038/386698a0.
Norwegian Centre for Climate Services. (n.d.). Meterological Data. Https://Seklima.Met.No/Observations/. Retrieved November 8, 2023, from https://seklima.met.no/Observations/.
Park, T., Ganguly, S., Tømmervik, H., Euskirchen, E.S., HØgda, K.A., Karlsen, S.R., Brovkin, V., Nemani, R.R., Myneni, R.B., 2016. Changes in growing season duration and productivity of northern vegetation inferred from long-term remote sensing data. Environ. Res. Lett. 11 (8) https://doi.org/10.1088/1748-9326/11/8/084001.
Phoenix, G.K., Bjerke, J.W., 2016. Arctic browning: extreme events and trends reversing arctic greening. In: Global Change Biology, Vol. 22, Issue 9. Blackwell Publishing Ltd., pp. 2960–2962. https://doi.org/10.1111/gcb.13261
Piao, S., Nan, H., Huntingford, C., Ciais, P., Friedlingstein, P., Sitch, S., Peng, S., Ahlström, A., Canadell, J.G., Cong, N., Levis, S., Levy, P.E., Liu, L., Lomas, M.R., Mao, J., Myneni, R.B., Peylin, P., Poulter, B., Shi, X., Chen, A., 2014. Evidence for a weakening relationship between interannual temperature variability and northern vegetation activity. Nat. Commun. 5 (1), 5018. https://doi.org/10.1038/ncomms6018.
Prach, K., Košnar, J., Klimešová, J., Hais, M., 2010. High Arctic vegetation after 70 years: a repeated analysis from Svalbard. Polar Biol. 33 (5) https://doi.org/10.1007/s00300-009-0739-6.
Rantanen, M., Karpechko, A.Yu., Lipponen, A., Nordling, K., Hyvärinen, O., Ruosteenoja, K., Vihma, T., Laaksonen, A., 2022. The Arctic has warmed nearly four times faster than the globe since 1979. Commun. Earth Environ. 3 (1), 168. https://doi.org/10.1038/s43247-022-00498-3.
Raynolds, M.K., Walker, D.A., Epstein, H.E., Pinzon, J.E., Tucker, C.J., 2012. A new estimate of tundra-biome phytomass from trans-Arctic field data and AVHRR NDVI. Remote Sens. Lett. 3 (5), 403–411. https://doi.org/10.1080/01431161.2011.609188.
Stendardi, L., 2020. Detection of Vegetation Phenology in Cold Regions Using a Combination of Radar and Optical Satellite Data. Free University of Bozen-Bolzano.
Tømmervik, H., Julitta, T., Nilsen, L., Park, T., Burkart, A., Ostapowicz, K., Karlsen, S.R., Parmentier, F.-J., Pirk, N., Bjerke, J.W., 2023. The northernmost hyperspectral FLoX sensor dataset for monitoring of high-Arctic tundra vegetation phenology and Sun-Induced Fluorescence (SIF). Data Brief, 109581. https://doi.org/10.1016/j.dib.2023.109581.
Tucker, C.J., 1979. Red and photographic infrared linear combinations for monitoring vegetation. Remote Sens. Environ. 8 (2), 127–150. https://doi.org/10.1016/0034-4257(79)90013-0.
van der Wal, R., Stien, A., 2014. High-arctic plants like it hot: a long-term investigation of between-year variability in plant biomass. Ecology 95 (12), 3414–3427. https://doi.org/10.1890/14-0533.1.
Vanderpuye, A.W., Elvebakk, A., Nilsen, L., 2002. Plant communities along environmental gradients of high-arctic mires in Sassendalen, Svalbard. J. Veg. Sci. 13 (6), 875–884. https://doi.org/10.1111/j.1654-1103.2002.tb02117.x.
Vickers, H., Høgda, K.A., Solbø, S., Karlsen, S.R., Tømmervik, H., Aanes, R., Hansen, B.B., 2016. Changes in greening in the high Arctic: insights from a 30 year AVHRR max NDVI dataset for Svalbard. Environ. Res. Lett. 11 (10) https://doi.org/10.1088/1748-9326/11/10/105004.
Walker, D.A., Raynolds, M.K., Daniëls, F.J.A., Einarsson, E., Elvebakk, A., Gould, W.A., Katenin, A.E., Kholod, S.S., Markon, C.J., Melnikov, E.S., Moskalenko, N.G., Talbot, S.S., Yurtsev, B.A.(†), The other members of the CAVM Team, 2005. The Circumpolar Arctic vegetation map. J. Veg. Sci. 16 (3), 267–282. https://doi.org/10.1111/j.1654-1103.2005.tb02365.x.
Walker, D.A., Kuss, P., Epstein, H.E., Kade, A.N., Vonlanthen, C.M., Raynolds, M.K., Daniëls, F.J.A., 2011. Vegetation of zonal patterned-ground ecosystems along the North America Arctic bioclimate gradient. Appl. Veg. Sci. 14 (4), 440–463. https://doi.org/10.1111/j.1654-109X.2011.01149.x.
Wang, J.A., Friedl, M.A., 2019. The role of land cover change in Arctic-Boreal greening and browning trends. Environ. Res. Lett. 14 (12), 125007 https://doi.org/10.1088/1748-9326/ab5429.
Xu, L., Myneni, R.B., Chapin III, F.S., Callaghan, T.V., Pinzon, J.E., Tucker, C.J., Zhu, Z., Bi, J., Ciais, P., Tømmervik, H., Euskirchen, E.S., Forbes, B.C., Piao, S.L., Anderson, B.T., Ganguly, S., Nemani, R.R., Goetz, S.J., Beck, P.S.A., Bunn, A.G., Stroeve, J.C., 2013. Temperature and vegetation seasonality diminishment over northern lands. Nat. Clim. Chang. 3 (6), 581–586. https://doi.org/10.1038/nclimate1836.